

Received April 3, 2020, accepted April 27, 2020, date of publication May 6, 2020, date of current version May 21, 2020.

Digital Object Identifier 10.1109/ACCESS.2020.2991846

Subpixel Computer Vision Detection Based on Wavelet Transform

YUYE FENG¹, TING YANG², AND YONGFENG NIU³

¹School of Mathematical Science, Zhejiang University, Zhejiang, Hangzhou 310000, China

²School of Science, Hangzhou Dianzi University, Zhejiang, Hangzhou 310000, China

³School of Science, Nanjing University of Aeronautics and Astronautics, Nanjing 210000, China

Corresponding author: Yuye Feng (11835030@zju.edu.cn)

ABSTRACT Computer vision detection technology is one of the most popular topics in the field of computer vision. With the continuous improvement of the relevant algorithm and the performance-price ratio of the corresponding imaging equipment, the corresponding computer vision detection algorithm is also constantly upgraded and deepened. Computer vision detection technology is mainly used in transportation, public security, national defense and military fields, but the pixel accuracy of traditional computer vision detection technology has been unable to meet today's accuracy requirements. In this paper, firstly, the quantum denoising algorithm based on dual-tree and dual-density wavelet transform is used to realize the combination of quantum image coding expression and wavelet transform, and finally achieve a more detailed and accurate description of the image and realize the noise reduction of the image. In order to further realize sub-pixel image processing, cubic spline interpolation edge detection algorithm will be added to wavelet transform, which mainly calculates the zeros of the second-order function corresponding to the cubic spline function on both sides of the image edge points, so as to realize sub-pixel location of the image edge points. Finally, by comparing with the traditional pixel accuracy detection algorithms, it can be found that the proposed sub-pixel computer vision detection algorithm based on wavelet transform has good robustness, and its computing time is relatively faster, so it will have better adaptability in practical applications.

INDEX TERMS Wavelet transform, vision detection algorithm, quantum denoising algorithm, subpixel vision detection algorithm.

I. INTRODUCTION

In the 21st century, with the continuous development of high-precision, cost-effective computer imaging hardware equipment and corresponding auxiliary detection algorithm, computer vision detection technology has become a research hotspot in various fields, especially in the military industry, computer vision detection technology is becoming more and more important in modern military industry [1]–[9]. The traditional computer vision detection technology has three important characteristics: non-contact, high precision and high automation. It can monitor objects independently and objectively, and measure and analyze their corresponding static and dynamic states [10]–[14]. But the traditional computer vision processing technology mostly depends on the computer hardware equipment and the corresponding digital image transmission and processing scheme. With the increas-

ing complexity of the image processed by the computer vision detection algorithm, the traditional image detection technology has been unable to meet the actual detection accuracy. Therefore, the research and analysis of higher accuracy and better computer vision detection algorithm appears. It is extremely important and meaningful [3], [15]–[17].

In order to solve the above problems, scholars and relevant research institutions around the world have done a lot of research and analysis on computer vision detection algorithms. Aiming at the image detection algorithm of wavelet transform, Bayram D and other relevant researchers [18]–[20] has proposed such algorithms as alternating projection maximum denoising algorithm and complex wavelet transform based on dual tree. This algorithm has the characteristics of good selectivity and simple computation complexity. Alfaroalmagro F and other relevant researchers [21]–[24] has proposed the nonlinear bivariate shrinkage function for the wavelet transform computer vision detection algorithm. When the above image denoising algorithms are applied in

The associate editor coordinating the review of this manuscript and approving it for publication was Zhihan Lv¹.

practice, the experimental results show that their edge preservation ability is poor. Aiming at the improvement of computer contactless visual inspection algorithm, Zhang H and other relevant researchers [25]–[27] has proposed a series of improved algorithms, such as basic matrix projective reconstruction, random consistency algorithm and incremental multi image 3D reconstruction algorithm, which can realize 3D reconstruction of detection images, but the corresponding detection accuracy can no longer meet the needs of realistic needs.

In order to further solve the problems of the above computer vision detection algorithm, the quantum denoising algorithm based on dual-tree dual-density wavelet transform is used to combine the quantum image coding expression with wavelet transform to achieve more detailed and accurate description of the image, and at the same time, denoising the image. In order to further realize sub-pixel image processing, Integrating cubic spline interpolation edge detection algorithm in wavelet transform, which mainly calculates the zeros of the second-order function corresponding to the cubic spline function on both sides of the image edge points, so as to realize sub-pixel location of the image edge points. Finally, by comparing with the traditional pixel accuracy detection algorithms, it can be found that the proposed sub-pixel computer vision detection algorithm based on wavelet transform has good robustness, and its computing time is relatively faster, so it will have better adaptability in practical applications.

The following arrangements will be made:

In the second section, we will analyze quantum denoising algorithm for sub-pixel image based on dual-tree and dual-density wavelet transform.

In the third section, we will analyze the cubic spline interpolation edge detection algorithm for sub-pixel image based on wavelet transform.

In the fourth section of this paper, the sub-pixel computer vision detection algorithm flow of wavelet transform and its corresponding system implementation will be analyzed and studied.

The last section of the article will summarize and outlook this article.

II. SUBPIXEL IMAGE CONSTRUCTION-QUANTUM DENOISING BASED ON DUAL-TREE DUAL-DENSITY WAVELET TRANSFORM

This section will mainly analyze and study one of the subpixel image construction algorithms proposed in this paper, which is based on the dual tree dual density wavelet transform. Meanwhile, this paper will analyze the transformation principle of the corresponding dual tree dual density wavelet transform and computer mechanism of quantum phase.

A. ANALYSIS AND RESEARCH OF DUAL-TREE AND DUAL-DENSITY WAVELET TRANSFORM

Dual-tree dual-density wavelet transform is mainly composed of dual-tree complex wavelet function and dual-density func-

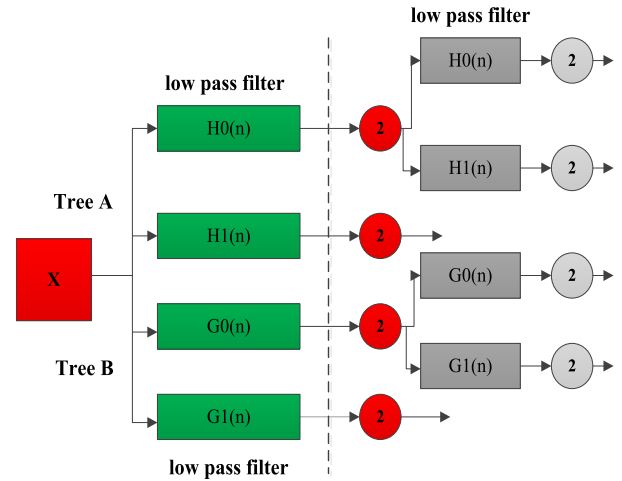


FIGURE 1. Wavelet transform decomposition filter diagram corresponding to dual-tree complex function.

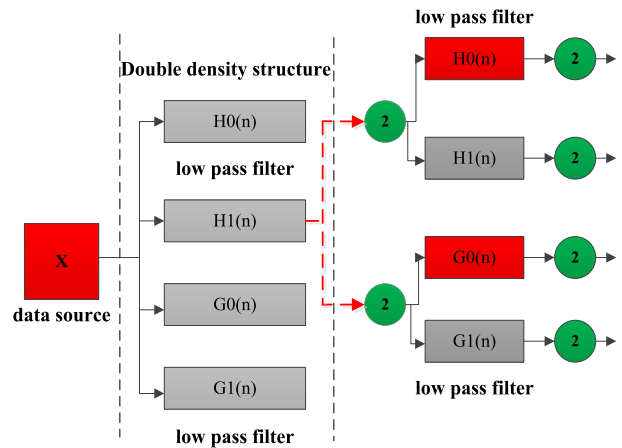


FIGURE 2. Schematic diagram of dual-density wavelet filter banks.

tion. Figure 1 shows the decomposition filter diagram of dual-tree complex function. The corresponding $H(n)$ represents the low-pass filter represented by the A tree in the double tree. The corresponding wavelet function is shown in formula 1, and the corresponding $H1(t)$ represents the high-pass filter of the corresponding A tree.

$$\psi(t) = \sqrt{2} \sum_n h_1(t) \varphi_h(2t - n) \quad (1)$$

The low-pass filter and high-pass filter corresponding to the corresponding B-tree in the dual-tree are the same as those corresponding to the A-tree, but the corresponding dual-tree filter needs to satisfy the following two requirements at the same time:

1. When sampling the wavelet signal, it needs to delay half a period of sampling and satisfy the delay characteristic of half sampling.

Two tree structures need to satisfy the characteristics of complete reconstruction, namely the so-called orthogonal property.

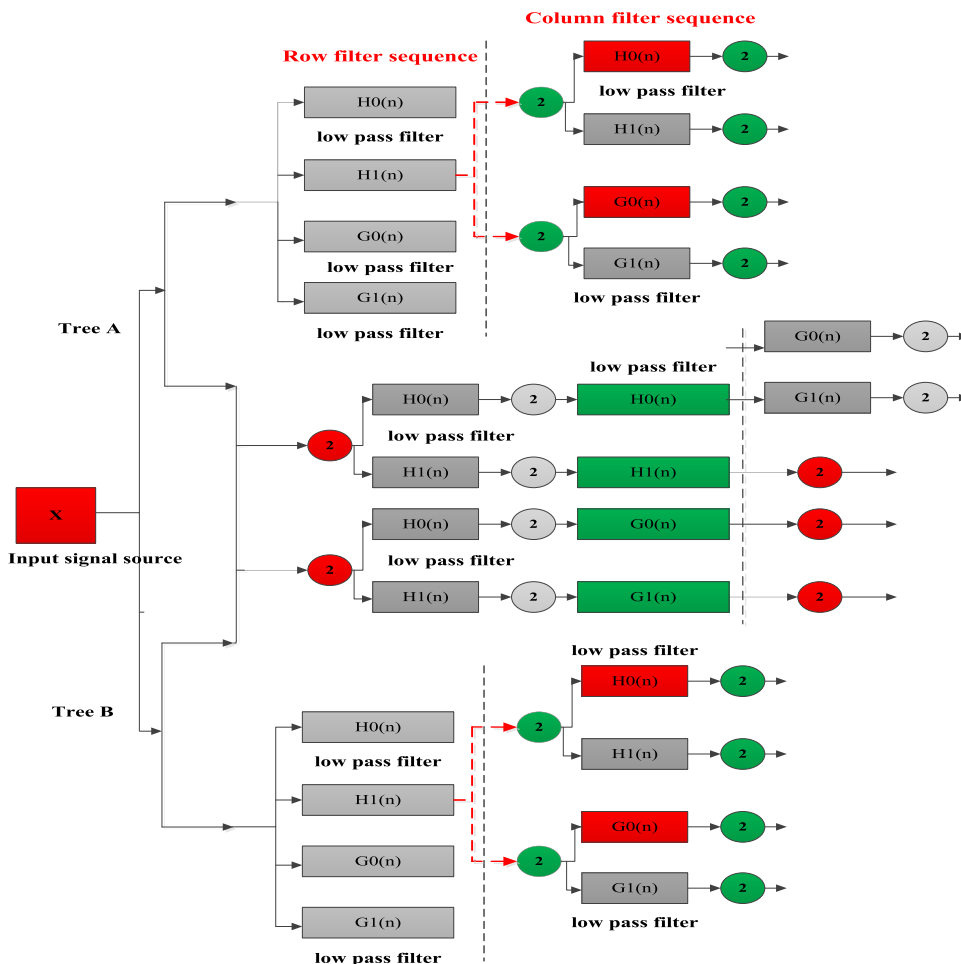


FIGURE 3. Diagram of dual-tree dual-density wavelet filter banks.

At the level of dual-density wavelet transform, the corresponding wavelet transform includes a scale function and two corresponding wavelet functions, and the corresponding offset of the two corresponding wavelet functions is 0.5. The corresponding scaling function and the corresponding calculation formulas of two wavelet functions are shown in formula 2, formula 3 and formula 4. The corresponding filters are $H_0(n)$, $H_1(n)$ and $H_2(n)$. The input signals are decomposed and reconstructed through the three filters mentioned above.

$$\psi(t) = \sqrt{2} \sum_n h_0(n) \varphi_h(2t - n) \tag{2}$$

$$\psi(t) = \sqrt{2} h_1(n) \varphi(2t - n) \tag{3}$$

$$\psi_2(t) \approx \psi_1(t - 0.5) \tag{4}$$

The corresponding double density wavelet filter bank schematic diagram is shown in Figure 2. The corresponding filter in the figure expands the corresponding one-dimensional double density wavelet transform in two dimensions and finally forms nine descendant coefficients.

In order to better realize the filtering of computer vision inspection image, the dual-tree dual-density function is combined to form the dual-tree dual-density complex wavelet

transform. Three Hilbert filter banks are used correspondingly. The corresponding filter banks have two scale functions and four resolution functions. The corresponding filter mainly uses low-pass filter, first-order high-pass filter and corresponding second-order high-pass filter. The corresponding two wavelet functions in the dual-tree double-density function are shown in the following formulas 5 and 6:

$$\psi_{h,1}(t) \approx \psi_{h,2}(t - 0.5) \tag{5}$$

$$\psi_{g,1}(t) \approx \psi_{g,2}(t - 0.5) \tag{6}$$

The approximate formula of the transformation between the two sets of wavelet functions is formulated as shown in formula 7:

$$\psi_{g,1}(t) \approx H \{ \psi_{h,1}(t) \}, \quad \psi_{g,2}(t) \approx H \{ \psi_{h,2}(t) \} \tag{7}$$

The corresponding dual-density dual-tree wavelet transform schematic diagram is shown in Figure 3, in which the corresponding architecture is a combination of A-tree and B-tree.

As shown in the figure 3, the high frequency information extracted by the real and imaginary wavelet coefficients of dual-tree dual-density wavelet transform corresponds to positive and negative 15 degrees, positive and negative 45 degrees and positive and negative 75 degrees in six directions. The

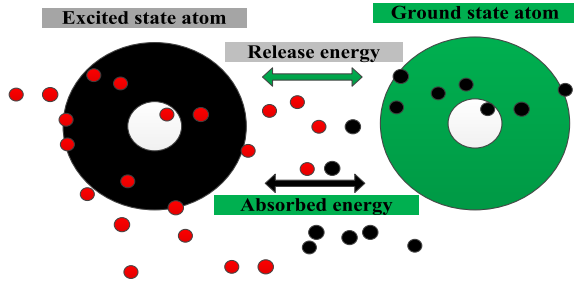


FIGURE 4. Conversion between ground and excited states of atoms in quantum theory.

corresponding characteristics of dual-tree and dual-density wavelet transform are as follows:

1. Translational invariance. The half-sampling delay between the corresponding filters implements the translation-invariant transformation of the signal, and the corresponding analysis results are position-independent.
2. It has the characteristics of continuous wavelet transform, which is different from discrete wavelet transform.
3. Multiple directional selectivity. The closer the description and fitting of the processing information is, the better the corresponding processing effect.
4. Anti-aliasing property.
5. Realize complete reconfiguration.
6. Computing complexity is low and the running time of the algorithm is short. The corresponding effect is obvious.

B. ANALYSIS OF HYBRID ALGORITHMS OF DUAL-TREE DUAL-DENSITY WAVELET TRANSFORM AND QUANTUM DENOISING

In order to better construct sub-pixel level computer vision detection technology, this paper adds quantum related denoising technology based on dual-tree dual-density wavelet transform. In this paper, we mainly use the principle of superposition of quantum states in quantum technology. Conventional quantum exists in two states, ground state and excited state. The corresponding transition process between ground state and excited state is shown in Figure 4.

The corresponding ground state and excited state in the quantum theory are regarded as the two corresponding states of noise and signal in the wavelet transform. The corresponding coefficients 0 and 1 represent the state of noise and the corresponding useful information respectively, and the wavelet coefficients are coded accordingly. In image quantum processing, it is assumed that the quantum system consists of two quantum states, corresponding to 0 state and corresponding 1 state. The corresponding four ground states will be generated as follows: formula 8, formula 9, formula 10 and formula 11.

$$|00\rangle = |0\rangle \otimes |0\rangle = \begin{pmatrix} 1 \\ 0 \\ 0 \\ 0 \end{pmatrix} \quad (8)$$

$$|01\rangle = |0\rangle \otimes |1\rangle = \begin{pmatrix} 1 \\ 0 \\ 0 \\ 1 \end{pmatrix} \quad (9)$$

$$|10\rangle = |1\rangle \otimes |0\rangle = \begin{pmatrix} 0 \\ 1 \\ 1 \\ 0 \end{pmatrix} \quad (10)$$

$$|11\rangle = |1\rangle \otimes |1\rangle = \begin{pmatrix} 0 \\ 1 \\ 0 \\ 1 \end{pmatrix} \quad (11)$$

Then the corresponding three primary colors of the image processed by computer vision are expressed by quantum expression as shown in formula 12.

$$\begin{aligned} |R\rangle &= |C_{XY}^0 C_{XY}^1 C_{XY}^2 \dots C_{XY}^7\rangle \\ |G\rangle &= |C_{XY}^8 C_{XY}^9 C_{XY}^{10} \dots C_{XY}^{15}\rangle \\ |B\rangle &= |C_{XY}^{16} C_{XY}^{17} C_{XY}^{18} \dots C_{XY}^{23}\rangle \end{aligned} \quad (12)$$

The corresponding processing mode of dual tree and double density wavelet transform based on quantum technology is shown in Figure 5 below. From the graph, we can see that its corresponding module is mainly composed of 6 modules, corresponding to image input module, adding noise module, quantum expression coding, wavelet denoising module, image reconstruction module and image output module.

III. CONSTRUCTION OF SUBPIXEL IMAGE-TRIPLE SPLINE INTERPOLATION EDGE DETECTION BASED ON WAVELET TRANSFORM

In order to further construct sub-pixel images and meet the requirements of computer vision detection, cubic spline difference edge detection algorithm is added to the wavelet transform to further assist image processing.

The equations corresponding to the cubic spline function are shown in equation 13.

$$\begin{bmatrix} 2 & A_0 & & \dots \\ B_1 & 2 & A_1 & \\ & B_2 & 2 & \\ & & \dots & \\ & & & \dots \\ & & & & \dots \\ & & & & & \dots \\ & & & & & & B_{n-1} & 2 & A_{n-1} \\ \dots & & & & & & & B_n & 2 \end{bmatrix} \begin{bmatrix} M_1 \\ M_2 \\ M_3 \\ \dots \\ \dots \\ \dots \\ M_{n-1} \\ M_n \end{bmatrix} = \begin{bmatrix} d_0 \\ d_1 \\ d_3 \\ \dots \\ \dots \\ \dots \\ d_{n-1} \\ d_n \end{bmatrix} \quad (13)$$

The corresponding parameters M0, M1, M2 and Mn are called boundary parameters, which are commonly called boundary conditions. The corresponding A0, A1 and An are called the corresponding system constants, and the corresponding B0, B1 and Bn are algebraic constants.

The corresponding edge detection principles are as follows:

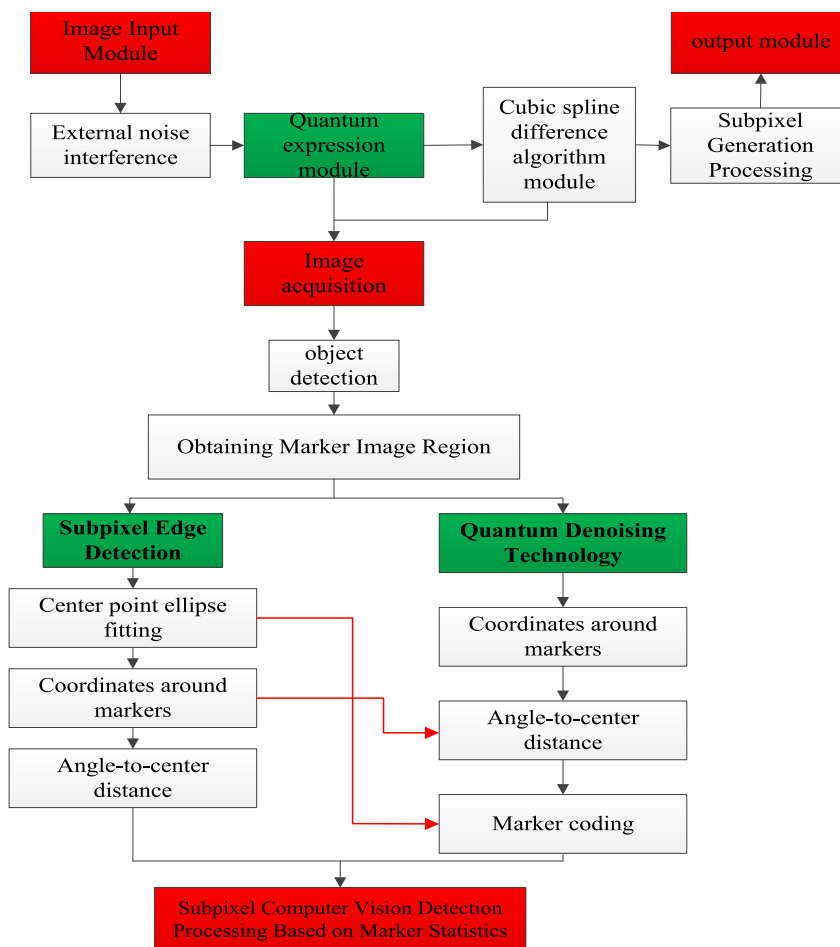


FIGURE 5. Flow chart of processing mode corresponding to dual-tree dual-density wavelet transform of quantum technology.

TABLE 1. Subpixel processing of wavelet transform based on cubic spline interpolation.

Processing steps	Handling details
Subpixel edge location	Integer pixel edge detection technology is used to realize sub-pixel edge location: gray value of edge region vector is calculated along the edge normal line.
Interpolation calculation based on cubic spline interpolation theory	Cubic spline interpolation theory for continuous edge gray distribution
Obtaining three-segment function and sub-pixel edge detection	By calculating the zero-crossing points of the second derivative of cubic polynomials on both sides of an integral pixel edge point, the possible positions and sums of two edges can be obtained. The location of the real edge point can be judged by using the defining fields of these two functions and the defining intervals of sub-pixel edge points, and the position can be chosen or rejected, thus realizing the edge location of sub-pixels.

Firstly, the corresponding nodes are selected according to the corresponding computer vision image, and the corresponding M pixels are selected in the corresponding nodes. The corresponding pixels meet the following requirements:

1. The y-axis values corresponding to the x-axis of the corresponding pixel coordinates should correspond one to one.
2. When the cubic spline interpolation function is used for the corresponding function, the difference formula is calculated in each sample interval, and the sub-pixel edge

location is carried out by using the maximum value of the first-order differential or the zero-crossing criterion of the second-order derivative. The corresponding linear algebraic equations are shown in formula 14. The corresponding m_0, m_1, m_{k-1} and m_n are all cubic spline interpolation functions. The corresponding A_0, B_k and C_n are constant values.

$$\begin{cases} 2m_0 + A_0m_1 = 0 \\ B_k m_{k-1} + 2m_k + A_k m_{k+1} = C_k, \quad (k = 1, 2, 3..n) \\ B_n m_{n-1} + 2m_n = C_n \end{cases} \quad (14)$$

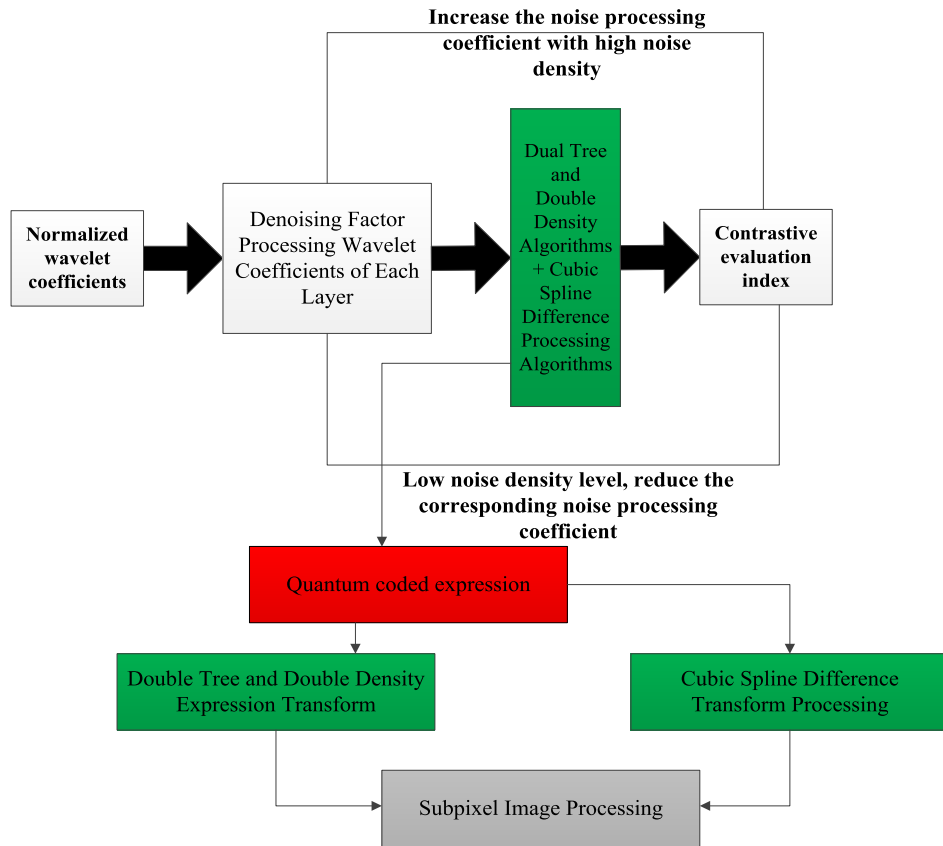


FIGURE 6. Flow chart of algorithm and detail diagram of core module.

After solving the above cubic spline interpolation function, the second order derivative of the cubic spline interpolation function is obtained and its derivative is 0. In the actual processing of image data, the corresponding processing steps are shown in Table 1 below.

IV. ALGORITHMIC FLOW AND SYSTEM IMPLEMENTATION OF SUB-PIXEL COMPUTER VISION DETECTION ALGORITHM BASED ON WAVELET TRANSFORM

Based on the sub-pixel computer vision processing technology of wavelet transform mentioned above, the sub-pixel processing of computer vision processing technology is realized by applying the dual-tree and double-density quantum noise reduction technology and the corresponding cubic spline interpolation processing technology in wavelet transform.

Based on the above theory, this paper builds a verification system, which is shown in Figure 6 as the flow chart of the corresponding algorithm and the detailed technical details of the corresponding core algorithm module. It can be seen from the figure that the processing details of the corresponding core module mainly focus on the process of decomposition and reconstruction.

On this basis, the traditional computer vision detection technology (Frost algorithm image, adaptive median filtering

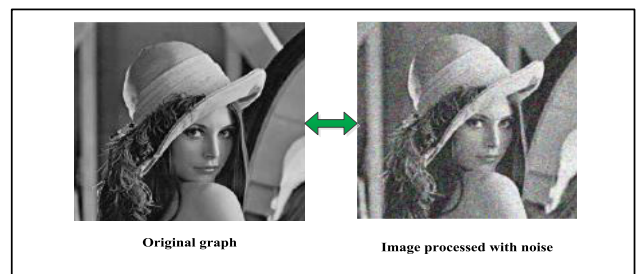


FIGURE 7. The original image and the image after adding noise.

algorithm and bilateral filtering algorithm) is compared. The main parameter of contrast is the noise reduction effect of corresponding image detection. In the actual experiment, the corresponding noise is added artificially in the corresponding effect picture, and the corresponding noise coefficients are Gaussian noise 0.1 and variance 0.2, respectively. When adding the noise in the actual experiment, the type of picture should be considered, and the Gaussian noise should be increased according to the type of picture. The case given in this paper is Unit8 format, which can be directly multiplied by a noise variance coefficient when adding the noise. The corresponding original image and noisy image are shown in Figure 7 [21].

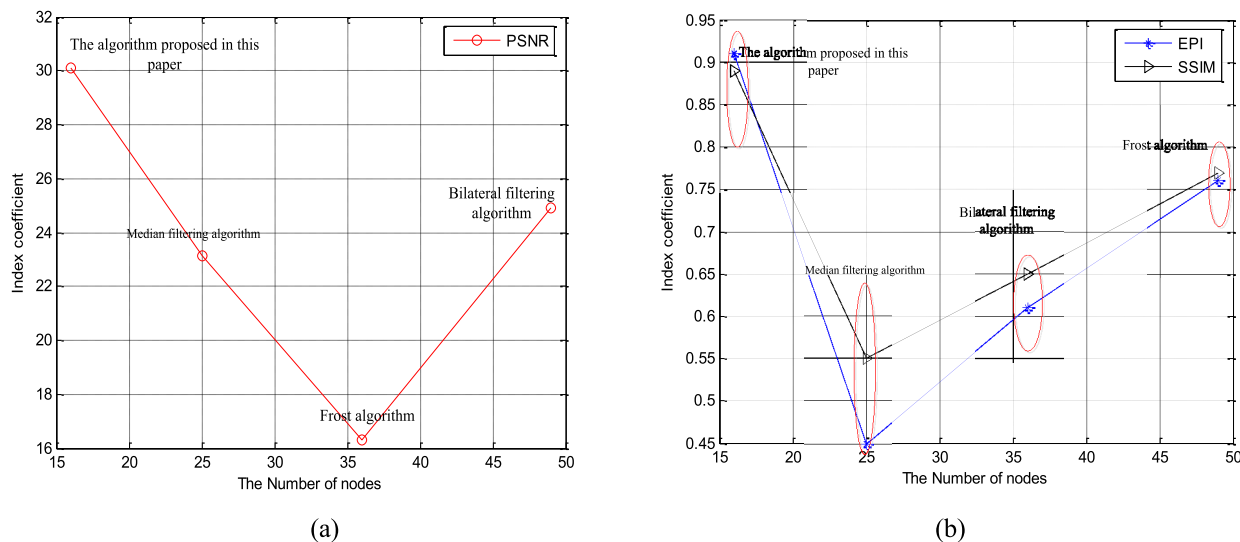


FIGURE 8. (a)(b). Three evaluation parameters (noise variance 0.1) polygraph based on four computer vision detection techniques.

TABLE 2. Evaluation parameters of four computer vision detection techniques (noise variance 0.1).

processing method	PSNR	Over percentage (%)	EPI	Over percentage (%)	SSIM	Over percentage (%)
The algorithm proposed in this paper	30.1134	--	0.91	--	0.89	--
Median filtering algorithm	23.1151	12.11	0.45	68.01	0.55	77.00
Frost algorithm	16.3267	74.12	0.61	47.21	0.65	34.51
Bilateral filtering algorithm	24.9176	11.34	0.76	18.11	0.77	14.62

After denoising the above images, the collected indicators are peak noise ratio (PSNR), edge preservation index (EPI) and structural similarity index coefficient (SSIM). The evaluation parameters of four kinds of computer vision detection techniques are shown in Table 2, and the corresponding broken-line graph is shown in Figure 8(a)(b). From the table, it is obvious that the proposed algorithm is superior to other algorithms in terms of peak-to-noise ratio, edge-preserving index and corresponding structural similarity. In order to compare parameters easily, the index EPI and SSIM in the graph are expanded 100 times, and are plotted in a graph with PSNR.

When the noise variance becomes 0.1, the evaluation parameters of the four computer vision detection technologies are shown in Table 3, and the corresponding broken-line graph is shown in Figure 9(a)(b). It is obvious from the table that the proposed algorithm is superior to other algorithms in terms of peak-to-noise ratio, edge-preserving index and corresponding structural similarity. In order to compare parameters easily, the index EPI and SSIM in the graph are expanded 50 times, and are plotted in a graph with PSNR. The corresponding PSNR calculation formula is shown in formula 15 below, where MSE is the mean square

error between the original image and the existing image, and Maxi is the maximum value of the image color.

$$PSNR = 20 \log_{10} \left(\frac{MAXI}{\sqrt{MSE}} \right) \quad (15)$$

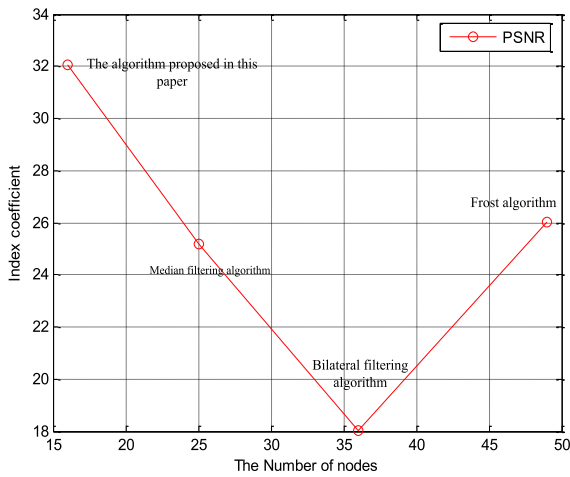
The results of the synthetic noise figure of 0.1 and 0.2 show that the corresponding comprehensive evaluation index broken line graph is shown in Figure 10. From the broken line graph, it can be seen that the corresponding algorithm proposed in this paper is superior to other algorithms about 10% in peak signal-to-noise ratio index, about 10% in edge preservation coefficient and 15% in structural similarity. In order to compare parameters easily, the index EPI and SSIM in the graph are expanded 100 times, and are plotted in a graph with PSNR.

V. SUMMARY AND PROSPECT

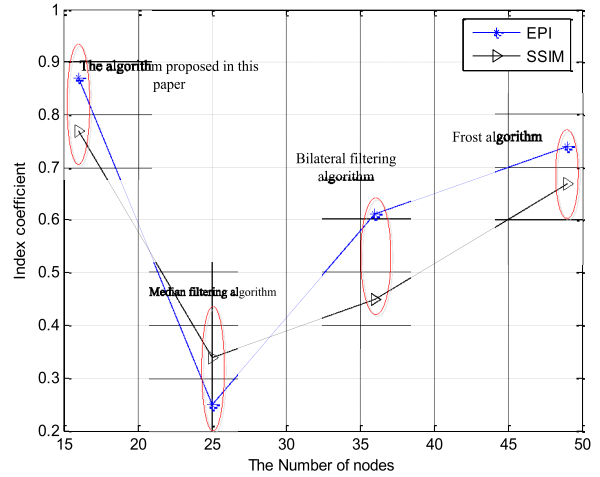
In this paper, the current research status of computer vision detection technology at home and abroad is analyzed in depth, and the application fields and corresponding application status of computer vision detection technology are discussed in detail. In view of the problems existing in the current computer vision inspection technology, this article has car-

TABLE 3. Evaluation parameters of four computer vision detection techniques (noise variance 0.2).

Processing method	PSNR	Over percentage (%)	EPI	Over percentage (%)	SSIM	Over percentage (%)
The algorithm proposed in this paper	32.0530	--	0.87	--	0.77	--
Median filtering algorithm	25.1702	15.02	0.25	69.05	0.34	76.00
Frost algorithm	18.0269	73.55	0.61	48.31	0.45	33.51
Bilateral filtering algorithm	26.0179	13.12	0.74	23.01	0.67	17.62



(a)



(b)

FIGURE 9. (a)(b). Three evaluation parameters (noise variance 0.2) polygraph based on four computer vision detection techniques.

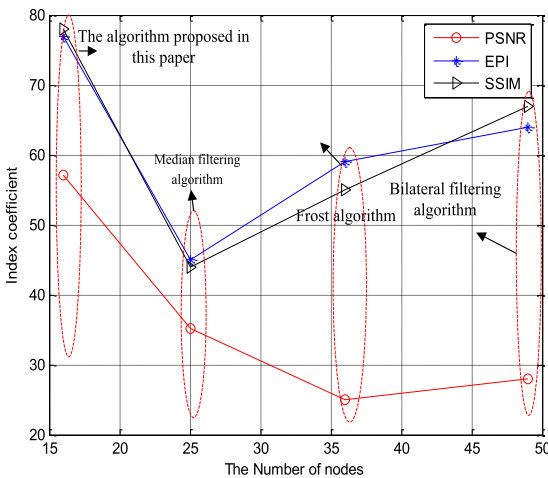


FIGURE 10. Three evaluation average parameters polygraph based on four computer vision detection techniques.

ried on the detailed analysis and discussion. At the same time, aiming at the problems summed up, this paper based on the dual tree dual density wavelet transform quantum de-noising algorithm, the quantum image coding expression

method and the wavelet transform are combined to achieve the more detailed and accurate description of the image, and at the same time, the image denoising processing is realized. In order to further realize sub-pixel image processing, a cubic spline interpolation edge detection algorithm is added to the wavelet transform, which mainly calculates the zeros of the second-order function corresponding to the cubic spline function on both sides of the image edge points, thus realizing the sub-pixel location of the image edge points. Finally, by comparing with the existing traditional pixel accuracy detection algorithms, it can be found that the proposed sub-pixel computer vision detection algorithm based on wavelet transform has good robustness, and its computing time is relatively faster, so it will have better adaptability in practical applications.

REFERENCES

[1] K. Nagarathinam and R. S. Kathavarayan, "Moving shadow detection based on stationary wavelet transform and zernike moments," *IET Comput. Vis.*, vol. 12, no. 6, pp. 787–795, Sep. 2018.
 [2] I. Kirbas and M. Peker, "Signal detection based on empirical mode decomposition and Teager-Kaiser energy operator and its application to P and S wave arrival time detection in seismic signal analysis," *Neural Comput. Appl.*, vol. 28, no. 10, pp. 3035–3045, Oct. 2017.

- [3] C. Choi, J. Park, H. Lee, and J. Yang, "Heartbeat detection using a Doppler radar sensor based on the scaling function of wavelet transform," *Microw. Opt. Technol. Lett.*, vol. 61, no. 7, pp. 1792–1796, Jul. 2019.
- [4] D. Hamidian, E. Salajegheh, and J. Salajegheh, "Irregular continuum structures damage detection based on wavelet transform and neural network," *KSCE J. Civil Eng.*, vol. 22, no. 11, pp. 4345–4352, Nov. 2018.
- [5] Z. Jakovljevic, R. Puzovic, and M. Pajic, "Recognition of planar segments in point cloud based on wavelet transform," *IEEE Trans. Ind. Informat.*, vol. 11, no. 2, pp. 342–352, 2nd Quart., 2017.
- [6] B. Ding and G. Wen, "Target recognition of SAR images based on multi-resolution representation," *Remote Sens. Lett.*, vol. 8, no. 11, pp. 1006–1014, Nov. 2017.
- [7] B. Dong, Z. Shen, and P. Xie, "Image restoration: A general wavelet frame based model and its asymptotic analysis," *SIAM J. Math. Anal.*, vol. 49, no. 1, pp. 421–445, Jan. 2017.
- [8] T. Wan, W. Zhang, M. Zhu, J. Chen, A. Achim, and Z. Qin, "Automated mitosis detection in histopathology based on non-Gaussian modeling of complex wavelet coefficients," *Neurocomputing*, vol. 237, pp. 291–303, May 2017.
- [9] S. Park, S. M. Lee, N. Kim, J. Choe, Y. Cho, K.-H. Do, and J. B. Seo, "Application of deep learning-based computer-aided detection system: Detecting pneumothorax on chest radiograph after biopsy," *Eur. Radiol.*, vol. 29, no. 10, pp. 5341–5348, Oct. 2019.
- [10] W.-M. Luo and Y.-R. Zhang, "Non-periodic pulse signal detection based on variable scale coupled duffing oscillators," *Electron. Lett.*, vol. 54, no. 5, pp. 280–281, Mar. 2018.
- [11] F. Zhang, T.-Y. Wu, and G. Zheng, "Video salient region detection model based on wavelet transform and feature comparison," *EURASIP J. Image Video Process.*, vol. 2019, no. 1, pp. 1–7, Dec. 2019.
- [12] M. Alemohammad, J. R. Stroud, B. T. Bosworth, and M. A. Foster, "High-speed all-optical Haar wavelet transform for real-time image compression," *Opt. Express*, vol. 25, no. 9, pp. 9802–9811, May 2017.
- [13] C. Vimalraj, S. Esakkirajan, T. Veerakumar, and P. Sreevidya, "Direction sensitive wavelet packet for despeckling of ultrasound images," *IET Comput. Vis.*, vol. 10, no. 7, pp. 746–757, Oct. 2016.
- [14] V. Gupta, T. Priya, A. K. Yadav, R. B. Pachori, and U. R. Acharya, "Automated detection of focal EEG signals using features extracted from flexible analytic wavelet transform," *Pattern Recognit. Lett.*, vol. 94, pp. 180–188, Jul. 2017.
- [15] J. Yang, Y. Wang, G. Wang, and M. Li, "Salient object detection based on global multi-scale superpixel contrast," *IET Comput. Vis.*, vol. 11, no. 8, pp. 710–716, Dec. 2017.
- [16] P. Vijayaraju, B. Sripathy, D. Arivudainambi, and S. Balaji, "Hybrid memetic algorithm with two-dimensional discrete Haar wavelet transform for optimal sensor placement," *IEEE Sensors J.*, vol. 17, no. 7, pp. 2267–2278, Apr. 2017.
- [17] H. Zhuang, K. Deng, Y. Yu, and H. Fan, "An approach based on discrete wavelet transform to unsupervised change detection in multispectral images," *Int. J. Remote Sens.*, vol. 38, no. 17, pp. 4914–4930, Sep. 2017.
- [18] D. Bayram and S. Seker, "Redundancy-based predictive fault detection on electric motors by stationary wavelet transform," *IEEE Trans. Ind. Appl.*, vol. 53, no. 3, pp. 2997–3004, May 2017.
- [19] G. S. Chen and Q. Z. Zheng, "Online chatter detection of the end milling based on wavelet packet transform and support vector machine recursive feature elimination," *Int. J. Adv. Manuf. Technol.*, vol. 95, nos. 1–4, pp. 775–784, 2017.
- [20] H. Tao and X. Lu, "Automatic smoky vehicle detection from traffic surveillance video based on vehicle rear detection and multi-feature fusion," *IET Intell. Transp. Syst.*, vol. 13, no. 2, pp. 252–259, Feb. 2019.
- [21] F. Alfaro-Almagro et al., "Image processing and quality control for the first 10,000 brain imaging datasets from UK biobank," *NeuroImage*, vol. 166, pp. 400–424, Feb. 2018.
- [22] Y. Zuo, Y. Wang, and X. Liu, "Adaptive robust control strategy for rhombus-type lunar exploration wheeled mobile robot using wavelet transform and probabilistic neural network," *Comput. Appl. Math.*, vol. 37, no. S1, pp. 314–337, 2017.
- [23] Z. Fan, D. Bi, L. He, M. Shiping, S. Gao, and C. Li, "Low-level structure feature extraction for image processing via stacked sparse denoising autoencoder," *Neurocomputing*, vol. 243, pp. 12–20, Jun. 2017.
- [24] F. Masoumi, T. Eslamkish, M. Honarmand, and A. A. Abkar, "A comparative study of Landsat-7 and Landsat-8 data using image processing methods for hydrothermal alteration mapping," *Resource Geol.*, vol. 67, no. 1, pp. 72–88, Jan. 2017.
- [25] H. Zhang, D. Zeng, H. Zhang, J. Wang, Z. Liang, and J. Ma, "Applications of nonlocal means algorithm in low-dose X-ray CT image processing and reconstruction: A review," *Med. Phys.*, vol. 44, no. 3, pp. 1168–1185, Mar. 2017.
- [26] C. Shi and L. Wang, "Remote sensing image compression based on adaptive directional wavelet transform with content-dependent binary tree codec," *IEEE J. Sel. Topics Appl. Earth Observ. Remote Sens.*, vol. 12, no. 3, pp. 934–949, Mar. 2019.
- [27] S. Baig, U. Ali, H. M. Asif, A. A. Khan, and S. Mumtaz, "Closed-form BER expression for Fourier and wavelet transform-based pulse-shaped data in downlink NOMA," *IEEE Commun. Lett.*, vol. 23, no. 4, pp. 592–595, Apr. 2019.



YUYE FENG was born in Anhui, China, in 1993. She is currently with the College of Mathematics and Science, Zhejiang University, Hangzhou, China. Since 2016, she has published two articles which included algebra and code.



TING YANG was born in Chongqing, China, in 1998. She is currently pursuing the bachelor's degree with Hangzhou Dianzi University. She is also with the College of Science, Hangzhou Dianzi University. Her research interests include algebra and code.



YONGFENG NIU is currently with the College of Computer Science and Technology, Nanjing University of Aeronautics and Astronautics, Nanjing, China, and the State Key Laboratory of Cryptology, Beijing, China.

...